THE JOURNAL OF PHYSICAL CHEMISTRY B

ARTICLE

pubs.acs.org/JPCB

Slow Threading Intercalation of Monomeric Ru(II) Complexes with 10,13-Diarylsubstituted dppz Ligands

Minna Li,[‡] Per Lincoln,[†] and Johanna Andersson*[,†]

[†]Department of Chemical and Biological Engineering, Chalmers University of Technology, SE-41296 Gothenburg, Sweden

[‡]School of Chemical Biology and Pharmaceutical Sciences, Capital Medical University, Beijing 100069, PR China

Supporting Information

ABSTRACT: Threading intercalation is an unusual DNA binding mode that displays extremely slow dissociation kinetics, which is an important feature for cytotoxicity, making threading intercalating compounds interesting as model compounds in the search for new DNA binding drugs. This type of binding has for ruthenium complexes previously only been observed for complexes containing 11-substituted dipyridophenazine ligands. In this work we have synthesized and investigated the DNA binding properties of two new 10,13-diarylsubstituted dipyridophenazine ruthenium complexes, using spectroscopic techniques, and found that this substitution pattern provides a new strategy for development of drugs with slow dissociation kinetics. However, the nature of the aryl substituents largely affects the binding properties of the complexes as it was found that a dithienyl substituted complex exhibit slow dissociation kinetics characteristic for threading intercalation while its diphenyl substituted analogue seems to bind DNA by partial intercalation of one phenyl substituent resulting in faster dissociation.

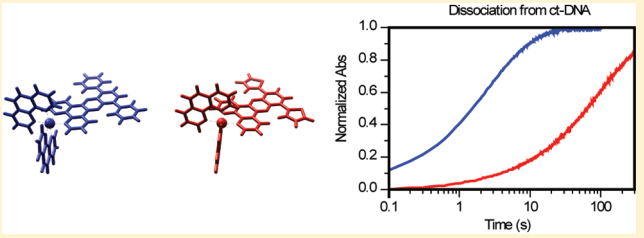

INTRODUCTION

Since the DNA binding properties of $[Ru(phen)_3]^{2+}$ (phen = 1,10-phenanthroline) were reported by Barton et al. in 1984,[1] ruthenium complexes have been intensively studied as conformational and photophysical probes for nucleic acids and as potential drug leads for chemotherapy.[2−5] Extending one of the phenanthroline ligands of $[Ru(phen)_3]^{2+}$ by fusing it with a quinoxaline to form a dipyridophenazine (dppz) ligand increased the DNA affinity and also introduced "light switch" properties to the complex, i.e., a bright luminescence when intercalated into DNA but almost completely quenched emission when free in aqueous solution.[6] Strong DNA affinity and slow dissociation rates, which are considered to be important for cytostatic activity,[7] could be further improved by the attachment of bulky substituents to C11 on the dppz moiety as exemplified by the binuclear dimer $[\mu\text{-bidppz}(phen)_4Ru_2]^{4+}$ (bidppz = 11,11′-bi-(dipyrido[3,2-*a*:2′,3′-*c*]phenazinyl)).

The slow kinetics of $[\mu\text{-bidppz}(phen)_4Ru_2]^{4+}$ has been ascribed to an unusual binding mode, where the two bulky ruthenium centers are found in opposite grooves of the DNA and the bridging ligand is intercalated between two base pairs, referred to as threading intercalation.[8] This type of binding was first observed for the cytotoxic natural product nogalamycin, which is an anthracycline antibiotic and thus constituted by four planar interconnected rings, but which in contrast to other anthracyclines has bulky sugar substituents in both ends of the ring system.[9−11] Since the discovery of the relationship between slow dissociation and cytotoxicity of DNA binding drugs, efforts have been made to develop new threading intercalators. This has resulted in the synthesis of a variety of DNA threading compounds, e.g., naphthalenediimide,[12−14] anthracenedione,[15] and acridine[16,17] based compounds with different bulky or charged substituents. There are also examples in the literature of compounds that specifically targets RNA[18,19] and quadruplex structures[20,21] by threading intercalation.

Common to all threading intercalators is that they display significantly reduced association and dissociation rates, compared to their nonthreading analogues, due to the fact that one of the charged or bulky substituents has to be threaded through the base pair stack for binding and dissociation to occur. Obviously, the threading process requires large distortions of the DNA helix structure, and in some cases probably even transient opening of at least one base pair. However, the rate constants for both association and dissociation vary greatly depending on the nature of the bulky substituents as well as the intercalating part. Most synthetic threading intercalators reported in the literature have dissociation rate constants on the order of $10^{1}-10^{-1}$ s^{-1},[12−16] and in comparison to those $[\mu\text{-bidppz}(phen)_4Ru_2]^{4+}$ display outstandingly slow dissociation with rate constants in the range $10^{-3}-10^{-4}$ s^{-1}, which is similar to the rate constants observed for nogalamycin.[7,8] The extremely slow kinetics in combination with favorable photophysical properties makes $[\mu\text{-bidppz}(phen)_4Ru_2]^{4+}$

Received: December 10, 2010
Revised: May 3, 2011
Published: May 25, 2011

Chart 1. Structures of the Two New $[Ru(phen)_2(dppz)]^{2+}$ Derivatives

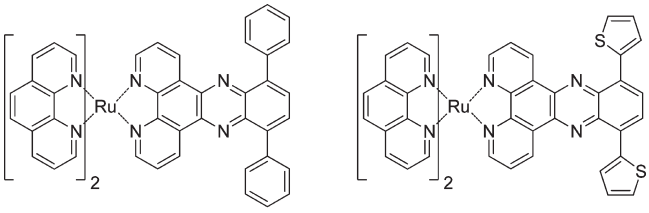

3-P 3-T

suitable as a model compound for threading intercalators, and several studies on this complex aiming for a deeper understanding of the mechanisms behind threading intercalation have been undertaken in our lab.[22−25]

Several different binuclear ruthenium complexes with varying auxiliary and bridging ligands have been synthesized after the discovery of the threading intercalating properties of $[\mu$-bidppz-$(phen)_4Ru_2]^{4+}$ to elucidate how complex structure affects threading intercalation ability, and it has been found that the nature of the ligands, as well as the chirality around the ruthenium centers, have a substantial effect on threading efficiency and sequence selectivity.[24,26,27] Recently it was also discovered that mononuclear ruthenium complexes with bulky quaternary ammonium substituents in the 11-position on the dppz moiety exhibit reduced intercalation rates.[28] These complexes are thought to bind DNA by the same mechanism as the binuclear DNA threading complexes with the ammonium group corresponding to one of the ruthenium centers. Dissociation kinetics were found to be approximately 1 order of magnitude faster than for $[\mu$-bidppz$(phen)_4Ru_2]^{4+}$, but still much slower than for the unsubstituted mononuclear reference compound. Furthermore, it was found that both the charge and the distance between the bulky substituent and the ruthenium center affected the intercalation kinetics. However, despite the structural variability among known threading intercalators, threading intercalation has for ruthenium complexes only been observed for complexes containing a dppz ligand with substituents in 11-position.

Clearly, extending the dppz complex by various bulky substituents in the 11-position affects the DNA dissociation kinetics, but what about substitution in the 10-position? Introduction of large substituents perpendicular to the dppz long axis could be expected to impair intercalation of the dppz ligand due to steric interactions with the DNA backbone. However, in this work we show that 10,13-disubstituted dppz ruthenium complexes (Chart 1) indeed intercalates DNA, and that the association and dissociation kinetics are strongly affected by small changes in the structure of the substituents. The results of this work may give further insight into the structure activity relationship for DNA threading intercalating compounds, which would be of value for future design of more efficient DNA binding drugs.

EXPERIMENTAL METHODS

General Information Synthesis. All reagents and solvents used in the synthesis of the ligands and complexes were purchased from Aldrich and used without further purification. Homochiral $Ru(phen)_2$(1,10-phenanthroline-5,6-dione) hexafluorophosphate was prepared by the method previously reported by Hiort et al.[29] ^{1}H-NMR spectra were obtained on a Varian UNITY-VXR 5000 (400 MHz) spectrometer, and chemical shifts are referenced to the chloroform peak (7.26 ppm) or the DMSO peak (2.5 ppm).

The synthetic route for preparation of **3-P** and **3-T** is shown in Scheme 1. The procedure for preparation of **1-P** and **1-T** is based on the strategy previously reported for the synthesis of disubstituted benzothiadiazoles.[30,31]

*Synthesis of 4,7-Diphenylbenzo[1,2,5]thiadiazole (**1-P**).* 4,7-Dibromobenzo[1,2,5]thiadiazole (294 mg, 1 mmol), phenylboronic acid (268 mg, 2.2 mmol), and $Pd(PPh_3)_4$ (200 mg, 0.17 mmol) were dissolved in dioxane/water 4:1 (20 mL) purged with N_2. The suspension was refluxed for 4 h, and the color changed from red into brown, and finally green. The reaction mixture was allowed to cool to room temperature before 40 mL of water was added. The product was extracted with CH_2Cl_2 (3 × 10 mL) and purified by silica gel column chromatography with hexane:ether (20:1) as eluent (200 mg, 70%). ^{1}H NMR δH (400 MHz, $CDCl_3$): 7.47 (2H, t, J = 7.2 Hz), 7.56 (4H, t, J = 7.2 Hz), 7.80 (2H, s), 7.97 (4H, d, J = 7.2 Hz).

*Synthesis of 4,7-Di(2′-thienyl)benzo[1,2,5]thiadiazole (**1-T**).* **1-T** was prepared according to the same procedure as **1-P** using 2-thienylboronic acid, and was obtained in 74% yield after purification by silica gel column chromatography with hexane:ether (15:1) as eluent. ^{1}H NMR δH (400 MHz, $CDCl_3$) 7.22 (2H, t, J = 4.0 Hz), 7.47 (2H, d, J = 5.2 Hz), 7.89 (2H, s), 8.13 (2H, d, J = 3.6 Hz).

*Synthesis of 1,2-Diamino-3,6-diphenylbenzene (**2-P**).* **2-P** was prepared from **1-P** according to the procedure previously described by Neto et al.[32] 4,7-Diphenylbenzo[1,2,5]thiadiazole (**1-P**) (57 mg, 0.2 mmol), $NaBH_4$ (11 mg, 0.3 mmol), and $CoCl_2 \cdot 6H_2O$ (10 mg, 0.04 mmol) were dissolved in EtOH (5 mL). The solution was refluxed for 3 h, and a black solid appeared with time. The mixture was cooled to room temperature and filtered. Water (15 mL) was added to the filtrate, and the product was extracted with ether (3 × 10 mL). The combined organic phase was dried over Na_2SO_4 and the solvent was evaporated, resulting in **2-P** as a yellow solid (44 mg, 85%). ^{1}H NMR δH (400 MHz, $CDCl_3$): 6.79 (s, 2H), 7.37 (t, 2H, J = 8.0 Hz), 7.45−7.49 (m, 8H).

*Synthesis of 1,2-Diamino-3,6-di(2′-thienyl)-benzene (**2-T**).* **2-T** was prepared from **1-T** according to the same procedure as **2-P** and was obtained in 80% yield. ^{1}H NMR δH (400 MHz, $CDCl_3$): 6.88 (2H, s), 7.14 (2H, t, J = 4.4 Hz), 7.19 (2H, d, J = 5.2 Hz), 7.38 (2H, d, J = 4.8 Hz).

*Synthesis of Δ-[Ru(phen)$_2$10,13-diphenyldipyridophenazine]$^{2+}$ (**3-P**).* **3-P** was prepared from **2-P** by the method reported by Hiort et al. for the synthesis of $[Ru(phen)_2dppz]^{2+}$.[29] A solution of 1,2-diamino-3,6-diphenylbenzene (**2-P**) (0.05 mmol, 10 mg) in CH_3CN (0.5 mL) was added dropwise with stirring to a solution of Δ-[$Ru(phen)_2$(1,10-phenanthroline-5,6-dione)]-$(PF_6)_2$ (0.025 mmol, 19 mg) in CH_3CN (0.5 mL) containing a drop of acetic acid. The color of the mixture changed from dark brown to dark red. The mixture was stirred in a boiling water bath for 10 min and then cooled to room temperature. The crude product was precipitated by aqueous NH_4PF_6 (10%) and filtered off, washed with water, dried, and purified by column chromatography on aluminum oxide (basic, activity grade 3) with CH_3CN as eluent. After evaporation of the solvent the product was dissolved in a small volume of CH_3CN and precipitated as the chloride salt by addition of tetra-*n*-butylammonium chloride in acetone. The resulting orange-red solid was filtered off and washed with acetone (13 mg, 45%). ^{1}H NMR δH (400 MHz, DMSO-d_6): 7.55−7.59

Scheme 1. Synthetic Route for the Two New Ruthenium Complexes

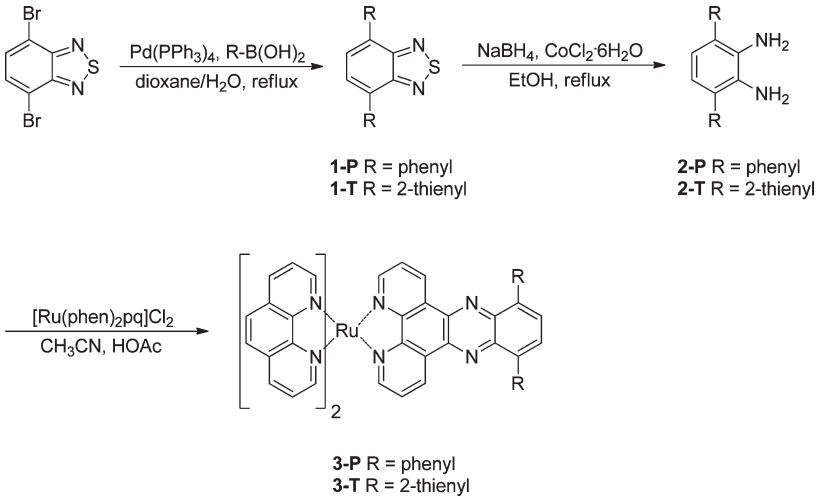

(m, 3H), 7.64−7.68 (m, 4H), 7.74−7.82 (m, 4H), 7.91 (t, 2H, J = 5.2 Hz), 7.97 (d, 3H, J = 8.4 Hz), 8.05 (d, 3H, J = 5.2 Hz), 8.18 (d, 2H, J = 4.8 Hz), 8.26 (d, 2H, J = 5.2 Hz), 8.35 (s, 2H), 8.40 (s, 4H), 8.78 (t, 3H, J = 8.0 Hz), 9.19 (d, 2H, J = 8.8 Hz).

*Synthesis of Δ-[Ru(phen)$_2$10,13-di(2′-thienyl)dipyridophenazine]$^{2+}$ (**3-T**).* **3-T** was prepared from **2-T** according to the same procedure as **3-P**, and was obtained in 52% yield after purification by column chromatography on aluminum oxide. ^{1}H NMR δH (400 MHz, DMSO-d_6): 7.35−7.59 (t, 2H, J = 4.8 Hz), 7.64−7.84 (m, 4H), 7.92 (d, 2H, J = 4.4 Hz), 8.03 (t, 2H, J = 6.4 Hz), 8.08 (d, 2H, J = 4.8 Hz), 8.21 (br, 2H), 8.24 (d, 2H, J = 5.2 Hz), 8.31 (d, 2H, J = 4.8 Hz), 8.41 (s, 4H), 8.74 (s, 2H), 8.80 (t, 4H, J = 8.0 Hz), 9.78 (d, 2H, J = 8.8 Hz).

The Λ enantiomers of **3-P** and **3-T** were prepared analogously from Λ-[Ru(phen)$_2$(1,10-phenanthroline-5,6-dione)](PF$_6$)$_2$.

Sample Preparation. A stock solution of ct-DNA was prepared by dissolving highly polymerized type I sodium salt calf thymus DNA (Sigma) in 150 mM NaCl buffer solution (1 mM sodium cacodylate, pH = 7.0) to a concentration of approximately 5−10 mM nucleotides. The solution was filtered three times through a 0.7 μm polycarbonate filter and diluted with 10 mM NaCl buffer solution (1 mM sodium cacodylate, pH = 7.0) to appropriate concentration. Stock solutions (∼5 mM nucleotides) of [poly(dAdT)]$_2$ and [poly(dGdC)]$_2$ were prepared by dissolving the sodium salts (Sigma) in 150 mM NaCl buffer solution, and were then diluted with 10 mM NaCl buffer solution to the desired concentrations. The [poly(dGdC)]$_2$ solution was heated at 50 °C for 45 min and then allowed to cool slowly to room temperature to obtain a homogeneous solution. Stock solutions of ruthenium complexes were prepared by dissolving the chloride salts of the complexes in 10 mM NaCl buffer solution. The DNA concentrations (in nucleotides) were determined spectrophotometrically using ε_{258} = 6600 M^{-1} cm^{-1} for calf thymus DNA, ε_{262} = 6600 M^{-1} cm^{-1} for [poly(dAdT)]$_2$, and ε_{254} = 8400 M^{-1} cm^{-1} for [poly(dGdC)]$_2$. The extinction coefficients for **3-T** and **3-P** were estimated to ε_{439} = 22 000 M^{-1} cm^{-1} and ε_{424} = 18 600 M^{-1} cm^{-1}, respectively, by comparison of the CD spectra in the UV region for both enantiomers with the CD of the corresponding enantiomers of [Ru(phen)$_2$dppz]$^{2+}$ at a concentration of 20 μM (ε_{439} = 20 000 M^{-1} cm^{-1} for [Ru(phen)$_2$dppz]$^{2+}$[29]). Samples were prepared by 1:1 mixing of DNA and complex solutions of appropriate concentrations except for the spectra in Figure 1 where a small volume of a concentrated (∼310 μM) complex stock solution in mQ was added to a larger volume of solvent or DNA solution to a final concentration of 10 μM.

Instrumentation. Circular dichroism (CD) spectra were measured on a JASCO J-810 CD spectropolarimeter using a 1 cm quartz cell. All spectra were baseline corrected by subtraction of the spectrum for the buffer only.

LD spectra were measured using a JASCO J-720 CD spectropolarimeter equipped with an Oxley prism to obtain linearly polarized light. The samples were oriented in a Couette cell with an outer rotating cylinder at a shear flow gradient of 3000 s^{-1}. All spectra were recorded at room temperature and baseline corrected by subtraction of the corresponding spectrum recorded without orientation. The association kinetics was studied by measuring the changes in the LD signal of the complex at 332 nm upon addition of ct-DNA. Dissociation was studied at 325 nm by addition of sodium dodecyl sulfate (SDS, 3% in 10 mM NaCl) to equilibrated samples of ruthenium complex and DNA in 10 mM NaCl to a final concentration of 0.6% SDS.

Absorption spectra were recorded on a Varian Cary 4000 UV/vis spectrophotometer. Association kinetics was studied by measuring the absorption intensity changes of the complex peak at 348 or 310 nm for **3-T** and **3-P**, respectively, upon addition of ct-DNA. Dissociation kinetics was studied at 25 °C with a Chirascan CD spectropolarimeter equipped with a stopped-flow device. SDS was mixed with equilibrated samples of ruthenium complex and DNA to a final concentration of 0.6% and the absorption change during 20, 100, or 300 s at 330, 317, or 373 nm for **3-T**, **3-P** and the dppz complex respectively was measured with the CD detector in the absorbance mode. In general 6 kinetic traces, obtained with the pressure hold function activated, were averaged and used for data fitting. All kinetic experiments were performed in 10 mM NaCl.

Data Analysis. DNA association and dissociation kinetic traces were projected on the space spanned by 1, 2, or 3 exponentials using the matrix pseudoinverse function *pinv* in the Matlab software package (Mathworks, Inc.). The (Euclidian)

dx.doi.org/10.1021/jp1117618 |J. Phys. Chem. B 2011, 115, 7923–7931

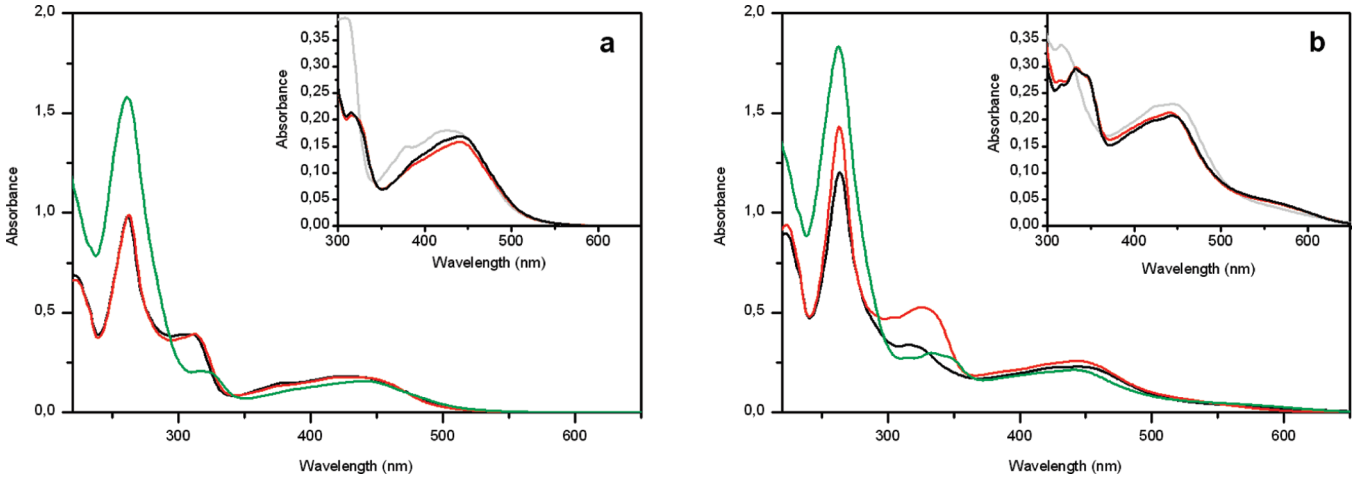

Figure 1. Absorption spectra of the Δ enantiomers of **3-P** (a) and **3-T** (b) in buffer (black), in MeOH (red), and in the presence of ct-DNA (green). The insets show the difference between the Δ (black) and Λ (red) enantiomers when bound to ct-DNA with the spectra of the complex free in buffer solution shown in gray. The concentrations of complex and ct-DNA are 10 and 120 μM, respectively.

norm of the residual was minimized by varying the rate constant with the simplex algorithm using the Matlab function *fminsearch*. A fit was judged acceptable if the residual was unstructured and inclusion of a further exponential did not decrease the residual norm by more than 30%. According to these criteria, 2 exponentials were needed to fit kinetic data for **3-T** and **3-P**, whereas 1 exponential was sufficient to fit the data for the dppz complex.

RESULTS

Absorption Spectroscopy. The absorption spectra of **3-P** and **3-T** in buffer solution, in MeOH, and in the presence of ct-DNA are shown in Figure 1. Despite the structural similarities between the two complexes, the shape of their absorption spectra in buffer solution differs substantially. The diaryl−dppz $\pi-\pi^*$ bands of **3-T** found at 315 nm and in the visible region are significantly shifted to the red compared to the corresponding absorption bands of **3-P**, and the intensity of the band at 315 nm is substantially lower for **3-T**. The hypochromicity observed for the 315 nm band of **3-T** is mainly an effect of aggregation, possibly by π-stacking, of the complex in buffer solution. This was confirmed by changing the solvent from buffer solution to methanol which significantly increased the intensity of the 315 and 260 nm bands of **3-T**, as shown in Figure 1b. No such observations were made for **3-P**, for which the spectrum was essentially unchanged on going from water to methanol as solvent (Figure 1a).

Comparison of the spectra of **3-P** in buffer and in the presence of DNA shows a slight hypochromicity in the MLCT band and the diaryl−dppz $\pi-\pi^*$ band in the visible region, and a more pronounced hypochromicity of the other diaryl−dppz $\pi-\pi^*$ band at 315 nm upon binding to DNA. Also, both $\pi-\pi^*$ bands exhibited a slight red shift upon addition of ct-DNA to the sample. As seen in the inset of Figure 1a, the hypochromicity in the visible region is slightly larger for the Δ enantiomer than for the Λ enantiomer.

Addition of ct-DNA to **3-T** resulted in a slight hypochromicity but no red shift in the visible region compared to the spectrum in buffer solution. The band at 315 nm on the other hand, displayed a substantial red shift but the hypochromicity was rather small compared to the pronounced intensity changes of the corresponding absorption band of **3-P**. However, as noted above, stacking of the complex in buffer solution was observed for **3-T**, and as a result the observed hypochromic effect upon binding to DNA is much smaller than the actual changes because the complex displays significant hypochromicity also in buffer solution. Comparison of the absorbances at 315 nm of the complex when bound to DNA and when in MeOH indicates a hypochromic shift of the same magnitude as observed for **3-P**. Contrary to what is observed for **3-P**, the hypochromicity in the visible region is slightly larger for the Λ enantiomer compared to the Δ enantiomer of **3-T** (inset Figure 1b).

Linear Dichroism and Reduced Linear Dichroism. The linear dichroism (LD) spectra of the two enantiomers of **3-P** and **3-T** bound to ct-DNA at equilibrium are shown in Figure 2. The Δ enantiomers show a slight positive peak around 420 nm, which is more prominent for the Λ enantiomers. Both enantiomers also display significant negative peaks around 320 and 330 nm for **3-P** and **3-T** respectively, as well as around 475 nm which for **3-T** shows a long tail toward the red end of the spectra.

The reduced linear dichroism (LD^r) is the LD divided by the isotropic absorption and from the LD^r the angle between the orientation axis (the DNA helix axis) and the transition dipole moment of the chromophore can be calculated. As can be seen in Figure 3, the LD^r spectra for the two complexes are remarkably similar to each other and also display great similarities, especially in the UV region, with the LD^r spectra of the parent complex $[Ru(phen)_2dppz]^{2+}$, which is a known DNA intercalator.[29] The differences in the visible can mainly be explained by the difference in the absorption spectra in this region. This result implies similar binding modes for the two new complexes as for the dppz complex.

This is also confirmed by a more detailed analysis of the LD and absorption spectra by calculation of the angles between the DNA helix axis and the B_E and B_{A2} polarized electronic transition dipole moments by the method previously used to determine the binding geometry of the dppz complex.[33,34] To obtain the binding geometry for the enantiomers of **3-T**, it was assumed that the substituents on the dppz ligand do not alter the orientation of the transition dipole moments within the molecule or the shape of the B_E and B_{A2} spectral components. The residual norm between the B_E and B_{A2} transitions for the dppz complex and **3-T** was minimized by varying the roll angle β for **3-T** using

dx.doi.org/10.1021/jp1117618 |*J. Phys. Chem. B* 2011, 115, 7923–7931

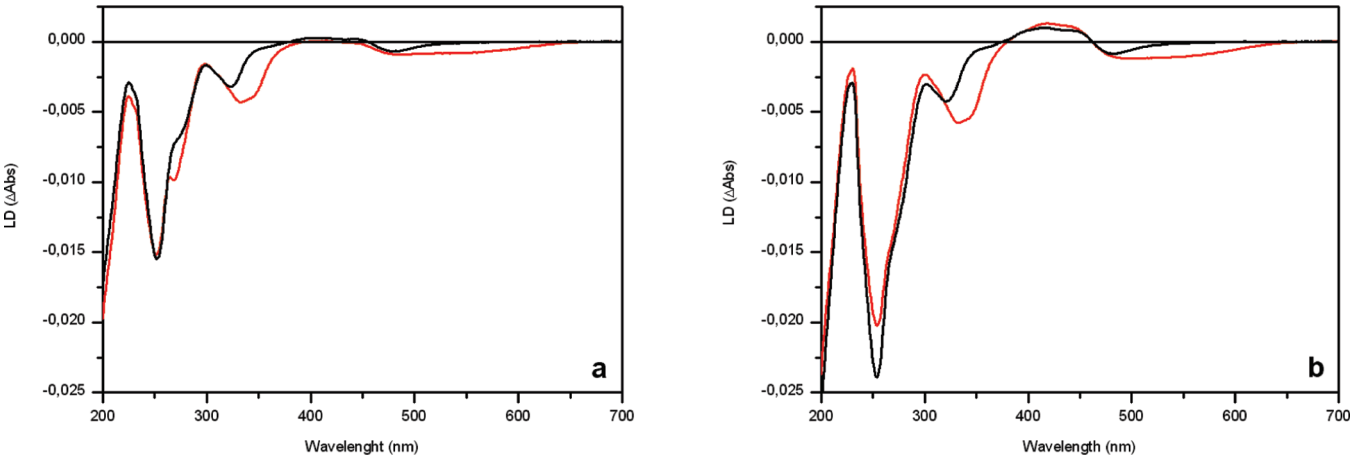

Figure 2. Linear dichroism spectra of the Δ (a) and Λ (b) enantiomers of **3-P** (black) and **3-T** (red). The concentrations of complex and DNA are 10 and 120 μM, respectively.

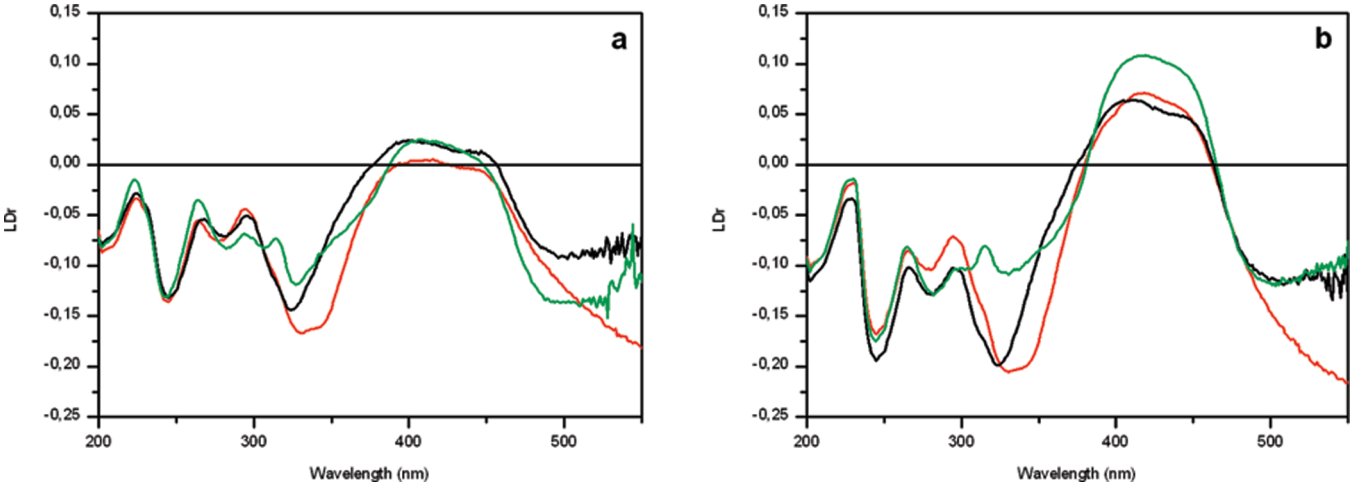

Figure 3. Reduced linear dichroism spectra of the Δ (a) and Λ (b) enantiomers of **3-P** (black), **3-T** (red), and the dppz complex (green) in presence of ct-DNA. The concentrations of complex and DNA are 10 and 120 μM, respectively.

the Matlab function *fminsearch*. This resulted in β values of +4° and +14° for Δ and Λ enantiomers of **3-T**, respectively, which are in excellent agreement with the values +7° and +13° reported for the Δ and Λ enantiomers of the dppz complex.[33] The spectral components for the B_E and B_{A2} transitions obtained for **3-T** with the binding angles above are virtually identical to the corresponding components of the dppz complex (Figure S1 in Supporting Information). The same approach for **3-P** yielded roll angles of +9° and −2° for the Δ and Λ enantiomers, respectively, though the difference between the B_E and B_{A2} spectral components of **3-P** and the dppz complex was slightly larger than for **3-T**.

Kinetics. Both enantiomers of **3-T** slowly change binding modes as seen by the dramatic change in the shapes of their LD spectra upon incubation at 50 °C (Figure S2 in Supporting Information). The kinetics of the process was studied by measuring the change in LD signal at 332 nm after addition of DNA to the complex (Figure S3 in Supporting Information). However, LD kinetic experiments are limited by the fact that a prolonged rotation of the Couette flow cell, used to obtain orientation of the samples, might damage the DNA resulting in decreased orientation of the sample. Therefore, due to the slow kinetics, the whole binding process could not be studied by LD but instead absorption spectroscopy was used for a more thorough investigation of the association kinetics. The kinetic traces from the absorption experiments are shown in Figure 4, and it can be seen that binding of both enantiomers of **3-T** did not reach steady state until after 10 h at 25 °C. From Figure 4 it is also evident that the association of the Λ enantiomer is slower than for the Δ enantiomer. For **3-P**, no major changes in the shape of the LD and absorption spectra with time were observed, indicating that equilibrium is reached virtually immediately after mixing the samples.

The dissociation kinetics was studied by addition of SDS to a final concentration of 0.6% w/w to equilibrated samples of complex and ct-DNA. The dissociation traces of both enantiomers of the two complexes, measured by stopped-flow with absorption detection at 25 °C in 10 mM NaCl, are shown in Figure 5. Both enantiomers of **3-T** display very slow dissociation kinetics and were also studied by conventional absorption spectroscopy to view the whole dissociation process to the final state, because the final state was not reached within the 300 s of

dx.doi.org/10.1021/jp1117618 |*J. Phys. Chem. B* 2011, 115, 7923–7931

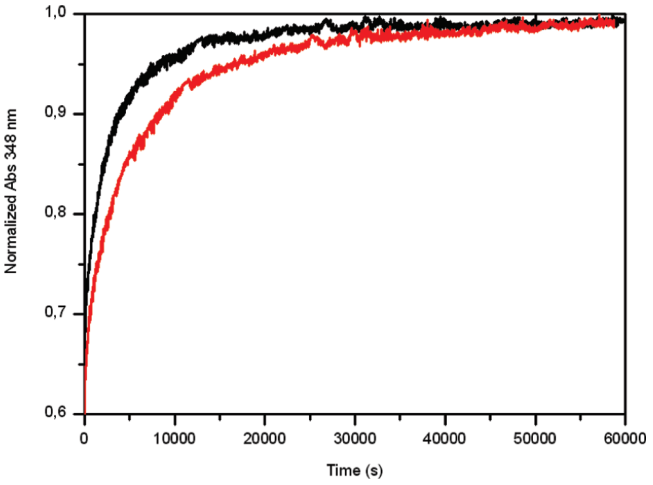

Figure 4. Association kinetics of the Δ (black) and Λ (red) enantiomers of **3-T** studied by absorbance at 348 nm. The measurement was made at 25 °C with 10 μM complex, 120 μM ct-DNA, and 10 mM NaCl.

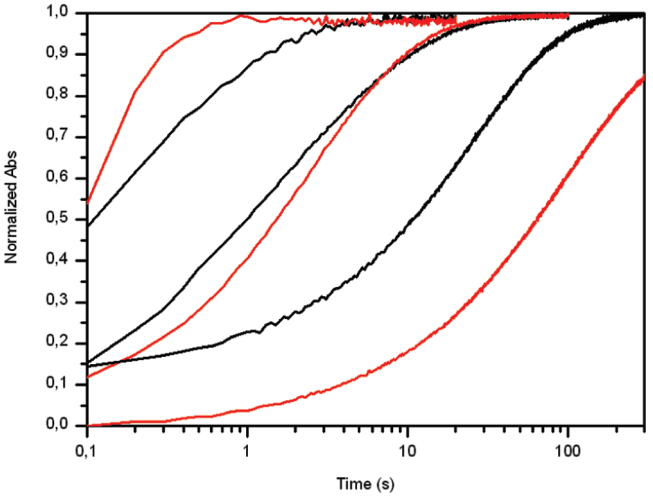

Figure 5. Dissociation kinetics of the Δ (black) and Λ enantiomers (red) of all three complexes studied by stopped-flow with absorbance detection at 25 °C and 10 mM NaCl. Dissociation was initiated by mixing a stock solution of 3% SDS with equilibrated samples of ct-DNA (120 μM) and ruthenium complex (10 μM) to a final concentration of 0.6% SDS. The order from left to right is $[Ru(phen)_2dppz]^{2+}$, **3-P**, and **3-T**.

the stopped-flow experiments (Figure S4 in Supporting Information). A sum of two exponentials was used to fit the kinetic traces and the rate constants are presented in Table 1.

The dissociation rates for **3-T** are approximately 1−2 orders of magnitude faster than for the well studied $[\mu$-bidppz-$(phen)_4Ru_2]^{4+}$,[8] though it is still very slow compared to the disocciation of both enantiomers of the dppz complex, which were used as references here, indicating a significant barrier for dissociation to occur. **3-P** displays faster dissociation rates than **3-T**, but the dissociation is still slower than for the dppz complex. Interestingly, both enantiomers of **3-P** display very similar dissociation traces, whereas **3-T** and the dppz complex show large differences between the enantiomers. Monitoring the dissociation by LD spectroscopy yielded dissociation kinetic traces

Table 1. Rate Constants for SDS Induced Dissociation of Ruthenium Complexes from ct-DNA at 25 °C

sample[a]	k_1 [10^{-2} s^{-1}] (α_1)	k_2 [10^{-2} s^{-1}] (α_2)
Δ **3-T**	10 (0.33)	2.5 (0.67)
Λ **3-T**[b]	2.2 (0.38)	0.42 (0.62)
Δ **3-P**	90 (0.59)	12 (0.41)
Λ **3-P**	63 (0.56)	14 (0.44)
Δ-$[Ru(phen)_2dppz]^{2+}$	140	
Λ-$[Ru(phen)_2dppz]^{2+}$	890	

[a] Dissociation kinetics was studied by addition of a stock solution of 3% SDS to equilibrated samples of 10 μM complex and 120 μM ct-DNA to a final concentration of 0.6% SDS. The experiments were performed in 10 mM NaCl. [b] The rate constants for Λ **3-T** were determined from kinetic traces measured by conventional absorbance because steady state was not reached within the 300 s of the stopped-flow experiments. All other rate constants were determined from stopped-flow experiments.

similar to those when absorption spectroscopy was used for **3-T** and **3-P** (Figure S5 in Supporting Information), whereas the dissociation kinetics of the dppz complex was too fast to be studied with manual mixing of the sample.

Association and dissociation kinetics of **3-T** and **3-P** were also studied in presence of $[poly(dAdT)]_2$ and $[poly(dGdC)]_2$ by absorption spectroscopy (see Figure S6 in Supporting Information). No significant differences in association rates between the two synthetic polynucleotides and ct-DNA were observed for either of the complexes. Also the dissociation rates of **3-P** are similar for the three types of DNA. However, for **3-T** a large fraction of the complexes dissociates very fast from $[poly(dGdC)]_2$, though the dissociation rate of the remaining complexes is in the same range as for the two other types of DNA, indicating that only a small fraction of **3-T** binds $[poly(dGdC)]_2$ by threading intercalation. All kinetic traces for the synthetic polynucleotides were biexponential indicating that sequence heterogeneity cannot be the only cause of the two exponentials observed with ct-DNA.

DISCUSSION

The well studied ruthenium complex $[Ru(phen)_2dppz]^{2+}$ and its bipyridine analogue $[Ru(bpy)_2dppz]^{2+}$ have been suggested to bind ct-DNA by intercalation of the dppz ligand between the DNA base pairs based on the dramatic increase in luminescence and an unwinding angle of approximately 30° upon binding to DNA[6] as well as calculation of the binding geometry from LD data.[33,34] In this work the two enantiomers of $[Ru(phen)_2dppz]^{2+}$ have been used as references to determine the binding mode of the two newly synthesized aryl substituted dppz complexes.

The LD and LD^r spectra of the two new complexes bound to ct-DNA show great similarities with those of $[Ru(phen)_2dppz]^{2+}$. Hence, it seems likely that the two new complexes also bind DNA with the A polarized transition dipole moment (polarized along the 2-fold axis of the aryl substituted dppz ligand) more or less perpendicular to the helix axis. Calculations of the roll angles of the two new complexes bound to ct-DNA yielded results similar to those for parent dppz complex, though the Λ enantiomer of **3-P** deviates slightly from the other Λ enantiomers with a somewhat negative roll angle. However, all calculated values are consistent with intercalation of the diarylsubstituted dppz ligand between the base pairs.

In contrast to the similar binding geometries determined by the analysis of steady state LD spectra, kinetic experiments reveal a significant difference between **3-T** and **3-P**. **3-T** display very slow dissociation kinetics compared to the dppz complex, whereas the dissociation rate of **3-P** is between those of **3-T** and the dppz complex. There is also a difference in association rates where **3-P** seems to bind virtually immediately whereas binding of **3-T** is not completed until after 10 h at 25 °C. The propensity of **3-T** to aggregate in buffer solution may indeed influence the association rate, but it is unlikely to affect the dissociation rate. Hence, considering the slow dissociation of the complex from DNA, it is probable that also association is slow because the barrier to reach the bound state should be of the same magnitude as for the reverse process, though the exact numbers of the association rate constants reported here should be treated with caution. Altogether the kinetic data in combination with the LD results give a clear indication that the binding mode of **3-T** is threading intercalation. For **3-P** on the other hand, the experimental data are a bit more ambiguous.

In absence of NMR or crystallographic data of the DNA bound ligand, the reduced dissociation rates characteristic for threading intercalation has been used to distinguish threading intercalation from classical intercalation, but there are few reports in the literature on how slow the dissociation must be for the binding mode to be regarded as threading intercalation. Tanious et al. stated that dissociation rate constants are 10 s^{-1} or greater for classical intercalators and smaller than 5−6 s^{-1} for threading intercalators based on a study on anthracenedione compounds.[15] However, these criteria are clearly not applicable on ruthenium complexes because that would suggest that also the unsubstituted dppz complex binds DNA by threading intercalation, which is obviously not the case. Apparently, the cutoff between threading intercalation and classical intercalation varies for different classes of substances, and little research has been done in this area for ruthenium complexes. Therefore, it is difficult to judge whether the binding mode of **3-P** should be classified as threading or classical intercalation based on dissociation kinetic data. Consequently, there are two possible binding modes for **3-P** considering the LD results: partial intercalation, where a part of the dppz ligand and one of the phenyl substituents is stacked between the base pairs, or threading intercalation, where the dppz ligand is stacked with the base pairs and the phenyl substituents are found in the opposite groove relative the ruthenium center, but which have a significantly lower barrier for binding and dissociation compared to other threading intercalating ruthenium complexes.

Both binding modes mentioned above are consistent with LD data because LD is only dependent on the angle between the orientation axis and the transition dipole moments of the chromophore but not the distance between the chromophore and the DNA helix axis. However, the small but significant difference in roll angles obtained for **3-P** from the spectral deconvolution may be better explained by a partial intercalation binding mode; if the complex is bound by partial intercalation of the dppz ligand and a phenyl substituent, it is conceivable that is has a slightly larger conformational freedom compared to a complex bound by threading intercalation where the dppz ligand is fully inserted between the base pairs. Moreover, despite the reduced dissociation rate for **3-P** compared to the dppz complex, there are indications from the kinetic experiments that suggests that the binding mode of **3-P** is not threading intercalation. First, the association of **3-P** is very fast, which is usually not the case for threading intercalation because the barrier to pass the bulky substituents through the base pair stack during binding should be of the same magnitude as for dissociation. Second, the two enantiomers of **3-P** have very similar dissociation kinetics while there is a clear distinction in dissociation rates between the enantiomers of **3-T** and the dppz complex. Because the distance between the aryl substituents and the ruthenium center is very short in both **3-P** and **3-T**, the phenanthroline ligands are expected to be in close contact with the DNA helix if the complexes are threaded into the DNA. Because DNA is chiral it is likely that the chirality around the ruthenium center affects the interactions between the phenanthroline ligands and the DNA, and therefore a difference in binding affinity is expected for the two enantiomers of the same complex. The observation of similar dissociation rates for the two enantiomers of **3-P** hence suggests that the phenanthroline ligands are not forced to be in close contact with the DNA helix in the bound state and a partial intercalation binding mode is more likely. Third, there are no significant differences in neither association nor dissociation rates for **3-P** in the presence of $[poly(dAdT)]_2$, $[poly(dGdC)]_2$, and ct-DNA. Usually, threading intercalating compounds display slower association and dissociation kinetics for GC-containing sequences compared to AT-containing sequences.[7,9,14] Though it can be argued that there are no significant differences in association and dissociation rates between the different types of DNA for threaded **3-T** either, it is obvious that a large fraction of **3-T** dissociates very fast from $[poly(dGdC)]_2$, which indicates that only a fraction of the complexes binds $[poly(dGdC)]_2$ by threading intercalation. Hence, threading of **3-T** into GC-sequences seems to be slightly impaired compared to AT-sequences, despite the similar association and dissociation rates for threading intercalating **3-T**. In light of the reasoning above we propose that **3-P** binds DNA by partial intercalation of one of the phenyl rings, and we believe that the reduced dissociation rate of **3-P** compared to the dppz complex is a result of a larger binding constant for **3-P** rather than threading intercalation, which is not unlikely considering the larger hydrophobic surface of **3-P**.

The difference in binding mode for **3-P** and **3-T** is quite surprising considering the structural similarities between the two complexes. However, the width (the distance between the outermost parts of the aryl substituents on the dppz ligand) of the diaryl−dppz ligand is slightly larger for **3-P** (13.6 Å, determined from PM3 geometry optimized structures in HyperChem) than for **3-T** (12.6 Å), which might explain why **3-P** cannot bind DNA by threading intercalation. Because the widths of the diaryl−dppz ligands are in the same range or slightly larger than the maximum size of an intercalation pocket[35] and the width of the major groove,[36] it is possible that the diphenyl substituted dppz ligand is too large to pass through the DNA base pair stack while **3-T** is just small enough to slide through.

The different widths of the aryl−dppz ligands do not explain why **3-T** does bind by threading intercalation, though. By definition, there must be a barrier for the complex to bind and dissociate from the DNA for the binding mode to be regarded as threading intercalation. It is of course possible that passing the thienyl substituted dppz ligand through the base pair stack requires large distortions of the DNA structure and hence it represents such a barrier, but it does not explain why it is more favorable to continue the insertion of the thienyl substituted dppz ligand through the base pair stack to the threaded state instead of just partially intercalate a thiophene ring as proposed for **3-P**. The most obvious explanation for this is that the

thiophene ring does not stack as well with the DNA bases as the phenyl ring does. Hence, if the binding process starts by insertion of the aryl substituent between the base pairs, it will stop there for **3-P** because the stacking interactions between the phenyl substituted end of the dppz ligand and the DNA bases are favorable enough to represent a minimum in free energy for the system, while for **3-T** it is more favorable to insert the dppz ligand even further so that the bases stack only with the dppz moiety itself and not with the thiophene ring, despite the conformational stress this probably induces in the DNA.

This difference in stacking ability could be due to the fact that the thiophene ring has a slightly smaller hydrophobic surface or that the sulfur in the thiophene ring alters the electron distribution in an unfavorable way. Another possibility is that the slightly larger van der Waals radius of sulfur (1.80 Å vs 1.70 Å for carbon[17]) is too large to fit into the intercalation pocket. It has been reported in the literature that substitution of sulfurs for the oxygens in a DNA intercalating compound makes it more prone to groove binding, though the authors suggest that this is an effect of the altered curvature of the crescent shaped molecule making it fit better in the minor groove rather than the sulfurs making intercalation unfavorable. It should be noted, though, that there are also examples in the literature of sulfur containing compounds that are suggested to bind DNA by intercalation, but it is not established which parts of the molecules intercalate the DNA.[37−39]

The biexponential dissociation kinetics of both **3-T** and **3-P** suggest that there are two different binding modes or two types of binding sites for each complex. However, the latter seems not likely because dissociation from $[poly(dAdT)]_2$ and $[poly(dGdC)]_2$, which has to be considered as rather homogenic polynucleotides, is also biexponential. Neither is it likely that the two exponentials correspond to one threaded intercalated and one partially intercalated binding mode for each complex, because both rate constants for **3-T** are much smaller than the two rate constants for **3-P**. Moreover, Fox et al. have shown that the pre-exponential factors for the biexponential dissociation of daunomycin from ct-DNA vary with SDS concentration,[7] and Westerlund et al. have found that SDS catalyzes the dissociation reaction,[40,41] which further complicates the picture. Thus, the origin of the two exponentials for **3-T** and **3-P** is unclear, and the reported dissociation rate constants may be larger than their true values due to SDS catalysis, but there is still a significant difference in dissociation rates between **3-T** and **3-P** indicating different binding modes for the two complexes.

Interestingly, the dissociation rate constants for the Λ enantiomer of the DNA threading complex **3-T** are in the same range as for the ammonium substituted mononuclear ruthenium complexes.[28] Despite the fact that the dissociation was shown to be dependent on the charge of the bulky group passed through the DNA base pair stack in the previous study, we here obtain similar dissociation rate constants for a complex with neutral bulky substituents as for complexes with +1 charged substituents. Hence, this work shows that the dissociation rate for DNA threading complexes is also largely affected by the structure and position of the bulky substituents and that decreasing the charge of threading intercalating compounds can be compensated for by structural changes.

CONCLUSION

The DNA-binding properties of two newly synthesized mononuclear diaryl substituted dppz ruthenium complexes have been investigated. We have found that thienyl substituents in the 10- and 13-position on the dppz ligand results in slow association and dissociation kinetics that is characteristic for threading intercalation, an unusual binding mode that has for ruthenium complexes previously only been observed for 11-substituted dppz complexes. Moreover, the thienyl substituted complex is the first ruthenium complex that is uncharged in one end but still binds DNA by threading intercalation despite the fact that it has been shown that charge plays an important role for this type of binding. However, small differences in the structure of the aryl substituents largely affect the binding properties; the diphenyl substituted analogue seems to bind DNA by partial intercalation of one of the phenyl groups rather than threading intercalation. This difference in binding modes could be due to either the fact that the diphenyl substituted dppz ligand is too wide to pass through the DNA helix or that the phenyl rings stacks so well with the DNA bases that there is no driving force for further insertion of the ligand to the threaded state once the phenyl ring is intercalated. Finally, we note that this substitution pattern provides a new strategy for development of DNA binding drugs with slow dissociation kinetics.

ASSOCIATED CONTENT

Supporting Information. The calculated spectral components for the reported roll angles, comparison of LD spectra of **3-T** immediately after mixing and at equilibrium, kinetic traces for association of **3-T** measured by LD, dissociation of **3-T** measured by absorption spectroscopy, dissociation of **3-T** and **3-P** measured by LD, and association and dissociation of **3-T** and **3-P** from $[poly(dAdT)]_2$ and from $[poly(dGdC)]_2$. Details for the spectral deconvolution from LD and absorbance. This material is available free of charge via the Internet at http://pubs.acs.org.

AUTHOR INFORMATION

Corresponding Author

*E-mail: johanna.andersson@chalmers.se. Telephone: +46317723855. Fax: +46317723858

ACKNOWLEDGMENT

This work was funded by the Swedish Research Council (VR). We gratefully acknowledge Dr. Ergang Wang for help with preparation of **1-T** and My Andréasson, high school student at Hvitfeldtska gymnasiet, Gothenburg, for the initial DNA binding studies on **3-T**.

REFERENCES

(1) Barton, J. K.; Danishefsky, A. T.; Goldberg, J. M. *J. Am. Chem. Soc.* **1984**, *106*, 2172–2176.
(2) Clarke, M. J. *Coord. Chem. Rev.* **2002**, *232*, 69–93.
(3) Levina, A.; Mitra, A.; Lay, P. A. *Metallomics* **2009**, *1*, 458–470.
(4) Metcalfe, C.; Thomas, J. A. *Chem. Soc. Rev.* **2003**, *32*, 215–224.
(5) Pierard, F.; Kirsch-De Mesmaeker, A. *Inorg. Chem. Commun.* **2006**, *9*, 111–126.
(6) Friedman, A. E.; Chambron, J. C.; Sauvage, J. P.; Turro, N. J.; Barton, J. K. *J. Am. Chem. Soc.* **1990**, *112*, 4960–4962.
(7) Fox, K. R.; Brassett, C.; Waring, M. J. *Biochim. Biophys. Acta* **1985**, *840*, 383–392.
(8) Wilhelmsson, L. M.; Westerlund, F.; Lincoln, P.; Norden, B. *J. Am. Chem. Soc.* **2002**, *124*, 12092–12093.

(9) Fox, K. R.; Waring, M. J. *Biochim. Biophys. Acta* **1984**, *802*, 162–168.
(10) Kersten, W.; Kersten, H.; Szybalski, W. *Biochemistry* **1966**, *5*, 236–244.
(11) Smith, C. K.; Davies, G. J.; Dodson, E. J.; Moore, M. H. *Biochemistry* **1995**, *34*, 415–425.
(12) Ohtsuka, K.; Komizo, K.; Takenaka, S. *J. Organomet. Chem.* **2010**, *695*, 1281–1286.
(13) Sato, S.; Nojima, T.; Waki, M.; Takenaka, S. *Molecules* **2005**, *10*, 693–707.
(14) Tanious, F. A.; Yen, S. F.; Wilson, W. D. *Biochemistry* **1991**, *30*, 1813–1819.
(15) Tanious, F. A.; Jenkins, T. C.; Neidle, S.; Wilson, W. D. *Biochemistry* **1992**, *31*, 11632–11640.
(16) Bourdouxhe-Housiaux, C.; Colson, P.; Houssier, C.; Waring, M. J.; Bailly, C. *Biochemistry* **1996**, *35*, 4251–4264.
(17) Martelli, A.; Jourdan, M.; Constant, J. F.; Demeunynck, M.; Dumy, P. *Bioorg. Med. Chem. Lett.* **2006**, *16*, 154–157.
(18) Krishnamurthy, M.; Gooch, B. D.; Beal, P. A. *Org. Biomol. Chem.* **2006**, *4*, 639–645.
(19) Gooch, B. D.; Krishnamurthy, M.; Shadid, M.; Beal, P. A. *ChemBioChem* **2005**, *6*, 2247–2254.
(20) Fedoroff, O. Y.; Salazar, M.; Han, H. Y.; Chemeris, V. V.; Kerwin, S. M.; Hurley, L. H. *Biochemistry* **1998**, *37*, 12367–12374.
(21) Haq, I.; Trent, J. O.; Chowdhry, B. Z.; Jenkins, T. C. *J. Am. Chem. Soc.* **1999**, *121*, 1768–1779.
(22) Nordell, P.; Jansson, E. T.; Lincoln, P. *Biochemistry* **2009**, *48*, 1442–1444.
(23) Nordell, P.; Westerlund, F.; Reymer, A.; El-Sagheer, A. H.; Brown, T.; Norden, B.; Lincoln, P. *J. Am. Chem. Soc.* **2008**, *130*, 14651–14658.
(24) Nordell, P.; Westerlund, F.; Wilhelmsson, L. M.; Norden, B.; Lincoln, P. *Angew. Chem., Int. Ed.* **2007**, *46*, 2203–2206.
(25) Wilhelmsson, L. M.; Esbjorner, E. K.; Westerlund, F.; Norden, B.; Lincoln, P. *J. Phys. Chem. B* **2003**, *107*, 11784–11793.
(26) Westerlund, F.; Nordell, P.; Blechinger, J.; Santos, T. M.; Norden, B.; Lincoln, P. *J. Phys. Chem. B* **2008**, *112*, 6688–6694.
(27) Andersson, J.; Li, M. N.; Lincoln, P. *Chem.—Eur. J.* **2010**, *16*, 11037–11046.
(28) Li, M.; Lincoln, P. *J. Inorg. Biochem.* **2009**, *103*, 963–970.
(29) Hiort, C.; Lincoln, P.; Norden, B. *J. Am. Chem. Soc.* **1993**, *115*, 3448–3454.
(30) Aldakov, D.; Palacios, M. A.; Anzenbacher, P. *Chem. Mater.* **2005**, *17*, 5238–5241.
(31) Zhang, X. L.; Yamaguchi, R.; Moriyama, K.; Kadowaki, M.; Kobayashi, T.; Ishi-i, T.; Thiemann, T.; Mataka, S. *J. Mater. Chem.* **2006**, *16*, 736–740.
(32) Neto, B. A. D.; Lopes, A. S.; Wust, M.; Costa, V. E. U.; Ebeling, G.; Dupont, J. *Tetrahedron Lett.* **2005**, *46*, 6843–6846.
(33) Lincoln, P.; Broo, A.; Norden, B. *J. Am. Chem. Soc.* **1996**, *118*, 2644–2653.
(34) Lincoln, P.; Norden, B. *J. Phys. Chem. B* **1998**, *102*, 9583–9594.
(35) Collier, D. A.; Neidle, S.; Brown, J. R. *Biochem. Pharmacol.* **1984**, *33*, 2877–2880.
(36) Bloomfield, V. A.; Crothers, D. M.; Tinoco, I. *Nucleic Acids. Structures, Properties and Functions*; University Science Books: Sausalito CA, 2000; p 90.
(37) Ester, K.; Hranjec, M.; Piantanida, I.; Caleta, I.; Jarak, I.; Pavelic, K.; Kralj, M.; Karminski-Zamola, G. *J. Med. Chem.* **2009**, *52*, 2482–2492.
(38) Jarak, I.; Kralj, M.; Piantanida, I.; Suman, L.; Zinic, M.; Pavelic, K.; Karminski-Zamola, G. *Bioorg. Med. Chem.* **2006**, *14*, 2859–2868.
(39) Li, Z. G.; Yang, Q.; Qian, X. H. *Tetrahedron* **2005**, *61*, 8711–8717.
(40) Westerlund, F.; Nordell, P.; Norden, B.; Lincoln, P. *J. Phys. Chem. B* **2007**, *111*, 9132–9137.
(41) Westerlund, F.; Wilhelmsson, L. M.; Norden, B.; Lincoln, P. *J. Am. Chem. Soc.* **2003**, *125*, 3773–3779.